Origin of giant difference between fluorescence, resonance, and nonresonance Raman scattering enhancement by surface plasmons

G. Sun
University of Massachusetts Boston, Boston, Massachusetts 02125, USA

J. B. Khurgin
Johns Hopkins University, Baltimore, Maryland 21218, USA

(Received 1 May 2012; published 19 June 2012)

Fluorescence, resonance, and off-resonance Raman spectroscopy are all precise and versatile techniques for indentifying small quantities of chemical and biological substances. One way to improve the sensitivity and specificity of these measurement techniques is to use enhancement of optical fields in the vicinity of metal nanoparticles. The degree of enhancement, however, is drastically different as Raman enhancement of 10 orders of magnitude or more has been consistently measured in experiment, while the enhancement of the seemingly similar process of fluorescence is typically far more modest. While resonance Raman scattering has the advantages of higher sensitivity and specificity when compared with the ordinary, nonresonant Raman process, its plasmon enhancement is far less spectacular. In fact, both fluorescence and resonance Raman measurements are subject to quenching when the molecule is placed too close to the metal surface. Such an effect, however, is completely absent from the normal nonresonant Raman process. In this work, we present an analytical model that reveals the physics behind the strikingly different orders of magnitude in enhancement that have been observed, provide a fundamental explanation for the quenching effect observed in fluorescence and resonance Raman but not in normal Raman, establish limits for attainable enhancement, and outline the path to optimization of all three processes.

DOI: 10.1103/PhysRevA.85.063410 PACS number(s): 33.50.Dq, 73.20.Mf, 52.38.Bv

I. INTRODUCTION

Metal nanoscale structures are known to enhance various optical properties of objects of similar or smaller dimensions placed in their vicinity. (We refer to these objects, whether they are atoms, molecules, or quantum dots, simply as molecules in this article.) The enhancement is usually understood as coupling with the collective free-electron oscillations in the metal called surface plasmons (SPs) that induce strong localized electric fields near the surface. In these strong fields such diverse optical properties as absorption, fluorescence [1–6], electroluminescence (EL), and various nonlinear properties including Raman scattering [7–15] get naturally enhanced, enabling potentially high-efficiency emitters, sensors, and photovoltaic devices. Extensive ongoing efforts devoted to plasmonically enhanced optical devices have yielded some spectacular results observed in the laboratories around the world, yet, at this time the only widespread practical application of plasmonics remains the one in surface-enhanced Raman scattering (SERS) sensing, first obtained as early as the 1970s [16]. Subsequent work [17] has compared the enhancements of normal (nonresonance) Raman, resonance Raman, and fluorescence and has observed degrees of enhancement that vary by many orders of magnitude among the three different processes. While all these processes can be viewed as having one incident photon absorbed as excitation and another photon of a lesser (Stokes-shifted) energy emitted, normal Raman enhancements of 10 orders of magnitude or more have been consistently measured by many groups, which has led to single-molecule detection [5–9], the enhancement of a seemingly similar process of fluorescence, however, is typically far more modest [18]. Recently, the dramatic difference in the fluorescence and Raman enhancements has been used to demonstrate that the resonance Raman scattering of dye molecules can be detected against the background of fluorescence [19,20] when the molecule is placed on the metal surface. For enhancement of fluorescence either from molecules or quantum dots, however, a spacer is always needed to separate them from the metal surface to prevent quenching from taking place [5,6]. The difference between enhancement rates of Raman and fluorescence has been generally attributed to the fluorescence lifetime quenching [21] near the metal surface and the absence of commensurate Raman quenching, but the latter fact has never been explained in a straightforward way. Early works [17,22] have developed a fully quantum mechanical theory of enhancement and, in conjunction with experiments [17], have predicted higher enhancement of normal Raman scattering relative to resonance Raman and fluorescence, but these theories do not connect explicitly the enhancement and quenching effects to the resonances with SP modes. Among the various theoretical models [23–25] developed to describe these effects through local field enhancement in metal nanostructures, Xu *et al*. [23] have considered both the surface-enhanced resonance Raman scattering and fluorescence, but have failed to include the internal nonradiative decay of the excited molecule in their theory, which can lead to orders-of-magnitude difference in the degree of fluorescence enhancement, as shown below. When it comes to estimation of the effect the prior works relied on numerical calculations with no simple way to gauge the effect via analytical expressions. The plasmonics community can benefit from revealing the physics underlying the observed fact that seemingly similar processes experience SP enhancement on a completely different scale. The goal of this paper is

to provide such a straightforward and accessible explanation as well as to outline ways for optimizing enhancement of fluorescence and Raman for sensing applications.

This work is based on a recently developed comprehensive model of enhancement of optical properties by metal nanoparticles [26], using which we have previously treated photoluminescence enhancement [27] by combining analytical models for light absorption and emission in the presence of isolated metal nanoparticles. The salient feature of our approach, often overlooked before, is the inclusion of all the competing radiative and nonradiative processes leading to the conclusion that the attainable enhancement is, above all, dependent on the original efficiency of the given optical process. For instance, only weak emitters can be strongly enhanced by SPs while strong emitters may end up quenched. In this work, we extend this model to include the effect of high-order SP modes [28] and apply it to fluorescence, resonance, and normal (nonresonance) Raman to demonstrate that emission into nonradiative higher-order modes does quench fluorescence and to a lesser extent may quench resonance Raman scattering, while it has no measurable effect on nonresonance Raman. Using the example of a gold nanosphere, we show that the size of the metal nanoparticle as well as the separation between the molecule and the metal sphere can be optimized for a maximum fluorescence enhancement depending on the absorption cross section at the excitation frequency $\sigma_{\rm abs}(\omega_{\rm ex})$, the original radiative efficiency $\eta_{\rm rad}(\omega_S)$ at the Stokes emission frequency ω_S. A similar optimization is also possible for resonance Raman scattering depending on the ratio of coherent time T_2 to the radiative lifetime $\tau_{\rm rad}$ of the molecular state that is resonantly excited at $\omega_{\rm ex}$. However, no such optimization is feasible for the nonresonance normal Raman process which always gets maximal enhancement at the metal surface, and in fact we show that the normal Raman enhancement is nothing but fluorescence in the limit of both $\sigma_{\rm abs} \to 0$ and $\eta_{\rm rad} \to 0$ and resonance Raman enhancement at $T_2/\tau_{\rm rad} \to 0$.

II. PROPERTIES OF SURFACE PLASMON MODES

As we have already mentioned, most theoretical works dedicated to optical-process enhancement in the proximity of metal objects either rely heavily upon numerical methods or require from the reader familiarity with the advanced concepts of the electromagnetic theory, such as Green's function. As a result, the physics of enhancement (and quenching) gets obscured behind intertwined calculations. In contrast, our approach has a clear demarcation between physics of enhancement and the simple math that serves only to establish the eigenmodes of the systems. Once the eigenmodes have been established, the enhancement of various optical processes is easily found using the most trivial algebraic equations. These equations can then be applied to different geometries, which makes our results valid for wide range on nanostructures as discussed near the end of this section.

In this work we use an example of a single metal nanosphere (Fig. 1) with a radius a being placed in a dielectric media with the dielectric constant ε_D that, under the electrostatic approximation valid for subwavelength structures $a \ll \lambda$, supports an infinite number of SP modes, each characterized by a Legendre polynomial of index l ranging from 1 to ∞ with

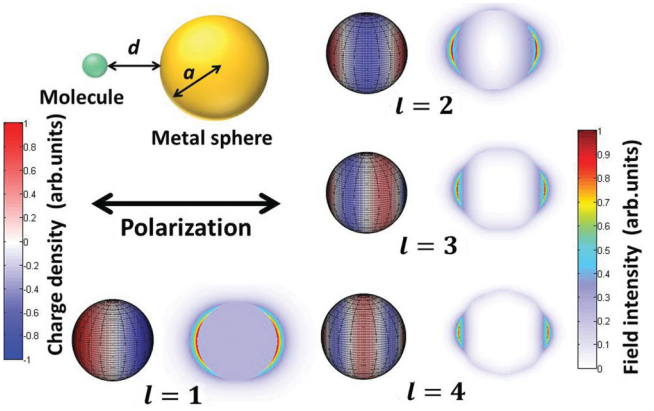

FIG. 1. (Color online) Illustration of the molecule placed at distance d from the surface of a single metal nanosphere of radius a, and the SP mode charge density (left) and field intensity (right) for the first four modes $l = 1, 2, 3, 4$.

resonant frequency ω_l defined by [26]

$$l\varepsilon_M(\omega_l) + (l+1)\varepsilon_D = 0, \tag{1}$$

where ε_M is the frequency-dependent dielectric function of metal. Using an analytical model [29] based on the properties for gold [30], we obtained the resonant SP mode energies for Au nanosphere surrounded by air ($\varepsilon_D = 1$) ranging from $\hbar\omega_1 = 2.562$ eV for the lowest-order (dipole) mode to $\hbar\omega_\infty = 3.468$ eV for the high-order modes [essentially equal to the energy of the surface plasmon polariton (SPP) propagating on the flat metal-air interface]. As illustrated in Fig. 1 (left in pair), only the $l = 1$ mode has positive and negative surface charges separately distributed on either the left or the right side of the sphere, yielding a nonzero dipole moment along the polarization; all higher-order modes with alternating positive and negative surface charges along the longitude horizontally connecting the two poles of the sphere where the electric field reaches its maximum value $E_{{\rm max},l}$ (right in pair) have vanishing dipole moment. As a result, all higher-order modes are uncoupled to the external fields for as long as the nanosphere diameter is much smaller than the wavelength, and it is only the $l = 1$ (dipole) mode that interacts with field with dipole moment that is proportional to the sphere volume (antenna effect), $p_1 = 2\pi a^3 \varepsilon_0 E_{{\rm max},1}$. This dipole mode therefore decays radiatively at a rate that is also proportional to the sphere volume [26],

$$\gamma_{\rm rad} = \frac{2\omega}{3\varepsilon_D}\left(\frac{2\pi a}{\lambda}\right)^3, \tag{2}$$

where λ is the wavelength in the dielectric. All higher-order modes $l > 1$ having zero dipole moment are uncoupled to the external fields. Simultaneously, all the modes also experience nonradiative decay due to the imaginary part of the metal dielectric function at roughly the same rate equal to the metal damping rate, $\gamma_{{\rm nrad},l} \approx \gamma$ [31], that is, on the order of 10 fs. The latter fact can be rather easily understood from a rather straightforward energy consideration in the electrostatic limit where the magnetic field vanishes when the size of the nanoparticle is significantly smaller than wavelength. The energy of each SP mode oscillates between potential and kinetic energy; when the phase is 0 or π the energy is entirely

in the form of potential energy of the surface charges, but when the phase changes to $\pi/2$ or $3\pi/2$ the energy has nowhere to go in the absence of the magnetic field but into the kinetic energy of moving electrons which do get scattered in the metal by defects and phonons. Thus, in a truly subwavelength structure, about half of the time all the energy is contained in the kinetic motion of electrons. Hence, on average, the energy loss rate is about one half of the energy loss rate in the metal 2γ, with little regard to any particular geometry or mode order. The decay rate can be summarized for all modes as

$$\gamma_l = \begin{cases} \gamma_{\rm rad} + \gamma, & l = 1, \\ \gamma, & l \geqslant 2. \end{cases} \tag{3}$$

Furthermore, as shown in Fig. 1, the SP mode energy (right in pair) is increasingly confined in a smaller region around the metal nanoparticle with the increase of mode index l. This is the consequence of positive and negative surface charges that alternate at greater spatial frequency for higher-order modes, effectively canceling electric field at progressively shorter distance away from the sphere. This confinement can be characterized by an effective volume defined through the mode energy $U_l = \frac{1}{2}\varepsilon_0\varepsilon_D E^2_{{\rm max},l} V_{{\rm eff},l}$ to arrive at [26]

$$V_{{\rm eff},l} = \frac{4\pi a^3}{(l+1)^2 \varepsilon_D}, \tag{4}$$

which is always less than the volume of the nanoparticle. Because the lower effective mode volume means higher field concentration, the inverse relationship of mode volume with the mode index l suggests higher-order nonradiative modes "hugging" the surface tend to interact more strongly with molecules that are closer to the surface but the strength of interaction falls off quickly away from the surface, which is exactly the origin of fluorescence quenching effect.

In this example of a highly symmetrical Au sphere, there exists a very strong degeneracy (three degenerate $l = 1$ dipole modes with three orthogonal polarizations, of which only one interacts with a given linearly polarized molecular dipole). If a more complicated design with lower symmetry is used, the degeneracies are lifted and mode mixing occurs. As a result, some of the higher-order modes acquire nonzero dipole moment and become partially radiating, as in various types of nanoantennae [2,4]. Qualitatively, however, the situation remains the same; the lower-order modes with larger effective volumes tend to have a substantial radiative decay component $\gamma_{\rm rad}$ and may thus contribute to the enhancement of radiative processes, while the higher-order modes with smaller effective volumes largely decay nonradiatively and can cause only quenching. Therefore, the following analysis will remain valid and the results will only be slightly modified for different shapes of the metal nanoparticle.

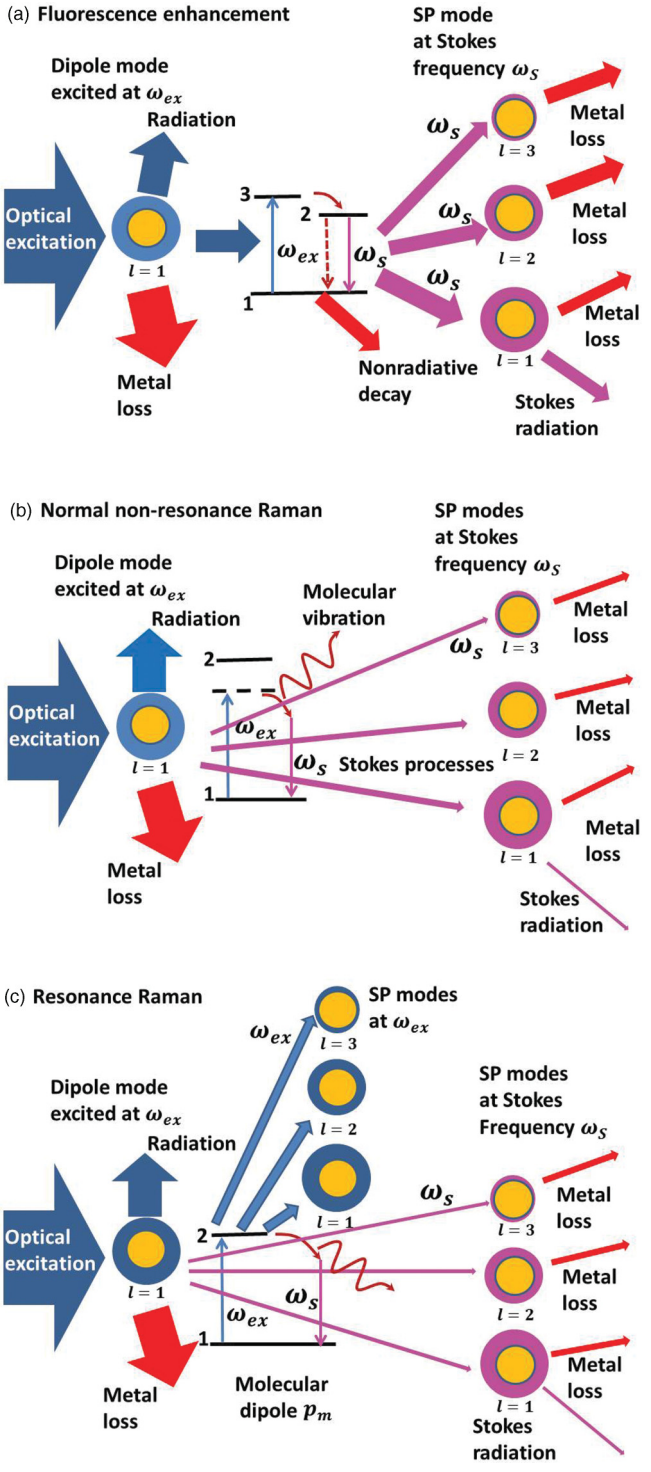

FIG. 2. (Color online) Illustration of energy flows in the enhancement processes of (a) fluorescence, (b) nonresonance Raman scattering, and (c) resonance Raman scattering.

III. FLUORESCENCE ENHANCEMENT

Let us now visualize the multistep fluorescence enhancement process, as illustrated in Fig. 2(a). First, the incident optical excitation of frequency $\omega_{\rm ex}$ is coupled exclusively into the dipole ($l = 1$) SP mode as all the higher-order ($l = 1$) modes have vanishing dipole moments and are not coupled with external fields. In the second step, a molecule placed at a distance d from the surface of the metal nanoparticle absorbs energy from this dipole mode at the rate $\gamma_{\rm abs} = \frac{c}{\sqrt{\varepsilon_D}} \frac{\sigma_{\rm abs}}{V_{{\rm eff},1}} (\frac{a}{a+d})^6$, where c is the speed of light in free space and $\sigma_{\rm abs}$ is the absorption cross section of the molecule, and simultaneously the molecule makes a transition from its ground state 1 to the excited state 3.

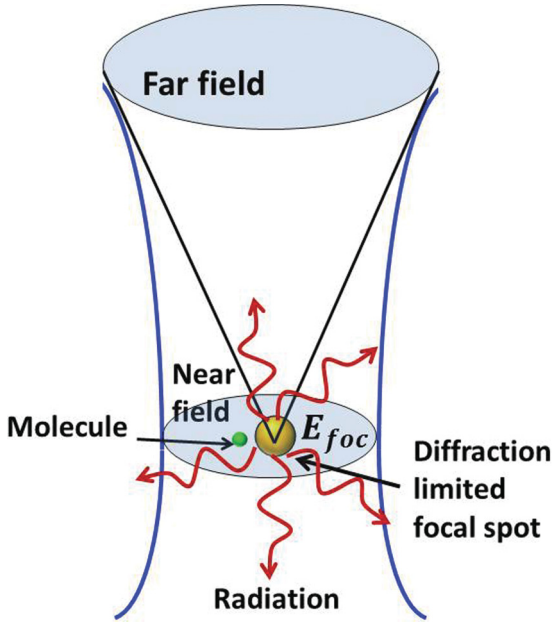

FIG. 3. (Color online) Illustration of a molecule situated in the surrounding SP field of the nanosphere placed at the diffraction-limited spot of a focused Gaussian beam ($E_{\rm foc}$ is the electric field at the focal spot in the absence of the metal sphere).

The enhancement of the absorption is estimated relative to the situation in the absence of metal, that is, when a Gaussian beam at the excitation frequency $\omega_{\rm ex}$ is focused onto a diffraction-limited spot with an electric field $E_{\rm foc}$, as shown in Fig. 3. In the presence of metal, the electric field of the dipole mode, $l = 1$, at the surface of the metal sphere being placed at the same focal spot is $E_{\max,1}$, and the absorption enhancement that is proportional to E^2 has been previously established as [26]

$$F_{\rm abs}(\omega_{\rm ex}) = \left|\frac{E_{\max,1}(\omega_{\rm ex})}{E_{\rm foc}}\right|^2\left(\frac{a}{a+d}\right)^6 = \frac{2\omega_{\rm ex}^2}{[\gamma_{\rm abs}+\gamma+\gamma_{\rm rad}]^2+4(\omega_{\rm ex}-\omega_1)^2}\left(\frac{a}{a+d}\right)^6. \tag{5}$$

As illustrated in Fig. 2(a), the denominator in Eq. (5) indicates that the energy stored in SP mode splits three ways, but typically the first term due to the molecular absorption is much smaller than the other two; hence, the enhancement of absorption does not depend on how strong the original absorption is in the molecule, except for the strongest of the absorbers.

Following absorption the molecule quickly relaxes nonradiatively to another excited state 2, typically characterized by a relatively long lifetime. Now, at step 3, all the energy stored in the state 2 splits into multiple decay channels, each characterized by its own decay rate. First of all there is a nonradiative relaxation with the rate $\tau_{\rm nrad}^{-1}$, and then there is decay at the Stokes-shifted frequency $\omega_s = \omega_{21}$ (wavelength of λ_S in the dielectric) into the lth SP mode at the rate $F_{P,l}\tau_{\rm rad}^{-1}$ enhanced by the Purcell factor $F_{P,l}$ relative to the original radiative decay rate of the molecule $\tau_{\rm rad}^{-1}$. The Purcell factor, inversely proportional to the effective mode volume $V_{{\rm eff},l}$, is the ratio of the density of states (DOS) of the lth mode to that of the free-space radiation modes and can be evaluated as [28]

$$F_{P,l}(\omega_S) = \frac{3\pi\varepsilon_D(l+1)^2\omega_S L_l(\omega_S)}{4}\left(\frac{\lambda_S}{2\pi a}\right)^3\left(\frac{a}{a+d}\right)^{2l+4}, \tag{6}$$

where the normalized Lorentzian line shape of the lth mode $L_l(\omega) = \frac{\gamma_l/2\pi}{(\omega-\omega_l)^2+\gamma_l^2/4}$ is determined by its decay rate γ_l given in Eq. (3). The small effective volumes of the high-order modes indicate that the energy can be coupled rather efficiently into these modes for sufficiently small separation d, but because they are uncoupled to the external fields the energy in the higher order modes simply dissipates in the metal. Hence, the higher-order modes present just another energy loss mechanism contributing nothing toward fluorescence emission, which is the origin of quenching. Only the dipole mode contributes to the fluorescence enhancement with an out-coupling efficiency $\eta_{\rm out} = \gamma_{\rm rad}/(\gamma_{\rm rad}+\gamma)$. Therefore, with the dipole mode acting as the only additional channel for the radiative decay, the total emission rate in the presence of the metal nanosphere,

$$\gamma_{\rm SP,rad} = \frac{1}{\tau_{\rm rad}} + \frac{F_{P,1}(\omega_S)}{\tau_{\rm rad}}\eta_{\rm out}, \tag{7}$$

while the total decay rate of the molecule is enhanced by SP modes of all orders as

$$\gamma_{\rm SP} = \frac{1}{\tau_{\rm rad}} + \frac{1}{\tau_{\rm nrad}} + \frac{1}{\tau_{\rm rad}}\sum_{l=1}^{\infty}F_{P,l}(\omega_S). \tag{8}$$

The emission stage of the enhancement can be obtained as the ratio of the radiative efficiency $\eta_{\rm SP} = \gamma_{\rm SP,rad}/\gamma_{\rm SP}$ in the presence of the metal nanosphere to the original radiative efficiency of the molecule $\eta_{\rm rad} = \tau_{\rm rad}^{-1}/(\tau_{\rm rad}^{-1}+\tau_{\rm nrad}^{-1})$ as

$$F_{\rm em}(\omega_S) = \frac{1+\eta_{\rm out}F_{P,1}(\omega_S)}{1+\eta_{\rm rad}\sum_{l=1}^{\infty}F_{P,l}(\omega_S)}. \tag{9}$$

Unlike Eq. (5) for absorption, the denominator of Eq. (9) contains terms of similar magnitude, indicating, as illustrated in Fig. 2(a) that emission into the many SP modes and nonradiative relaxation all compete for the fixed amount of energy stored in the excited state 2; thus, maximum emission enhancement and the distance at which it is obtained exhibits strong dependence on the original radiative efficiency $\eta_{\rm rad}$.

For the fluorescence process that consists of optical absorption at $\omega_{\rm ex}$ and emission at ω_S, the total enhancement is the product of the absorption and emission enhancement:

$$F_{\rm PL}(\omega_{\rm ex},\omega_S) = F_{\rm abs}(\omega_{\rm ex})F_{\rm em}(\omega_S) = \left|\frac{E_{\max,1}(\omega_{\rm ex})}{E_{\rm foc}}\right|^2\left(\frac{a}{a+d}\right)^6 \times \frac{1+\eta_{\rm out}F_{P,1}(\omega_S)}{1+\eta_{\rm rad}F_{P,1}(\omega_S)+\eta_{\rm rad}\sum_{l=2}^{\infty}F_{P,l}(\omega_{\rm PS})}. \tag{10}$$

The last term in the denominator is the emission into all the higher SP modes and represents the quenching that occurs when the molecule is placed in close proximity to the nanoparticle surface. The result of fluorescence enhancement for a molecule with $\sigma_{\rm abs} = 0.1$ nm^2 and $\eta_{\rm rad} = 0.01$ placed

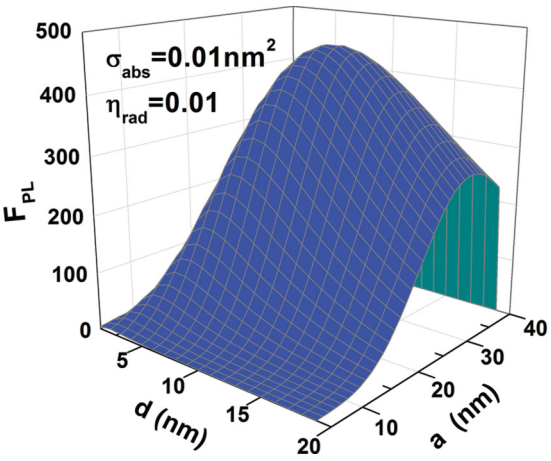

FIG. 4. (Color online) Fluorescence enhancement dependence on the Au nanosphere radius a and on the molecule-sphere separation d for a molecule with $\sigma_{\rm abs} = 0.1$ nm^2 and $\eta_{\rm rad} = 0.01$. The optical excitation is in resonance with the dipole mode $\omega_{\rm ex} = \omega_1 = 2.562$ eV, and the emission is at $\omega_S = 2.462$ eV.

in the vicinity of an Au sphere surrounded by air is shown in Fig. 4, where the optical excitation is assumed to be in resonance with the dipole mode $\hbar\omega_{\rm ex} = \hbar\omega_1 = 2.562$ eV, and the emission frequency is down-shifted by 100 meV to be at $\hbar\omega_S = 2.462$ eV.

We can see that the fluorescence enhancement factor exhibits strong dependence upon both the nanoparticle size and the separation between the molecule and particle. The optimal nanosphere size occurs at the radius where it is small enough to yield small effective mode volume for the sufficiently large field enhancement and Purcell factor, yet is still large enough to assure strong radiative coupling of the dipole mode for both excitation and emission. Without accounting for higher-order modes, it is always better to have molecules positioned as close as possible to the metal sphere in order to take advantage of the large Purcell factor as well as the strong field of the dipole mode. However, with high-order modes taken into account, the energy of the molecule placed too close to the metal sphere also gets coupled into these nonradiative modes and simply dissipates as metal loss. As a result, an optimized separation can be found to allow for significant coupling into the dipole mode while adequately suppressing the luminescence quenching by high-order modes.

IV. NONRESONANCE RAMAN ENHANCEMENT

We now turn our attention to the nonresonance Raman process as shown in Fig. 2(b). In comparison with the fluorescence process in Fig. 2(a), beyond the obvious similarity of both being a process in which one incident photon is absorbed and another photon at a different frequency is emitted, there is a dramatic difference: The excitation frequency for nonresonance Raman is, by default, far from any absorption resonance ω_m of the molecule. Once the optical excitation couples into the dipole mode, $l = 1$, in addition to the radiative and nonradiative decay, one dipole ($l = 1$) mode SP can also split into another lth-mode SP at the Stokes frequency ω_S and a quantum of molecular vibration with frequency $\omega_{\rm ex} - \omega_S$. The rate of spontaneous Raman scattering can be written following a Feynman diagram as [32]

$$\gamma_{\rm RM} = \frac{2\pi}{\hbar}\frac{|d_m E_{\rm ex}|^2}{\hbar^2(\omega_{\rm ex}-\omega_m)^2}\frac{|H_{\rm ev}|^2}{\hbar^2(\omega_S-\omega_m)^2}\frac{|d_m|^2\omega_S}{\varepsilon_0}\rho(\omega_S), \tag{11}$$

where ε_0 is the permittivity in vacuum, d_m is the dipole moment of the molecular transition, $E_{\rm ex}$ is the electric field experienced by the molecule, $H_{\rm ev}$ is the strength of electron-vibrational coupling responsible for the Raman process, and $\rho(\omega_S)$ is the effective DOS at the Stokes frequency ω_S. In the absence of nanosphere, $E_{\rm ex} = E_{\rm foc}$ is the electric field at the focal spot and $\rho(\omega_S)$ is simply the DOS of the radiation mode $\rho_{\rm rad}(\omega_S)$. Once the nanosphere is introduced not only does the excitation electric field $E_{\rm ex}$ get enhanced, but also the DOS near the nanosphere can be written as a sum of DOS for all SP modes, $\rho(\omega_S) = \sum_l \rho_l(\omega_S, d)$ and the Raman scattering occurs independently into each SP mode. As one can see from Fig. 2(b), in the absence of real molecular level (where it would go in the fluorescence process), the energy stored in the dipole SP mode at excitation frequency now directly splits between radiative decay ($\gamma_{\rm rad}$), metal loss (γ), and Raman scattering into multiple SP modes at Stokes frequency. Since the Raman rates are orders of magnitude weaker than either γ or $\gamma_{\rm rad}$, the amount of energy scattered via Raman process into the only "useful" $l = 1$SP mode is not affected at all by the Raman scattering into the higher-order modes (no quenching) and we can write the Raman enhancement for the same geometrical arrangement as in the fluorescence setup (Fig. 3), where the metal nanosphere is placed in the focal spot of a Gaussian beam as

$$F_{\rm RM}(\omega_{\rm ex},\omega_S) = \left|\frac{E_{\max,1}(\omega_{\rm ex})}{E_{\rm foc}}\right|^2\left(\frac{a}{a+d}\right)^6[1+\eta_{\rm out}F_{P,1}(\omega_S)]. \tag{12}$$

The main difference between Eq. (12) and Eq. (5) is the absence of the "energy splitting" denominator in Eq. (12) since there is no real state in the molecule from which the energy splitting (or branching out) can take place. Since the excitation of the nonresonance Raman process is far away from any of the molecular resonance, the Raman cross section is typically many orders of magnitude less than the absorption cross section $\sigma_{\rm abs}$ when it is excited close to its resonance; thus, the field intensity ratio $|\frac{E_{\max,1}}{E_{\rm foc}}|^2$ can be obtained from Eq. (5) by taking $\sigma_{\rm abs} \to 0$, or $\gamma_{\rm abs} \to 0$ and then it is not difficult to see that the Raman enhancement is equal to fluorescence enhancement in the limit of both $\sigma_{\rm abs} \to 0$ and $\eta_{\rm rad} \to 0$. For practical Raman enhancement measurement, the Raman process related to the dipole mode should always be much stronger than that of the radiation mode, $\eta_{\rm out}F_{P,1}(\omega_S) \gg 1$; thus, $F_{\rm RM} \propto |\frac{E_{\max,1}}{E_{\rm foc}}|^2 F_{P,1}(\omega_S)$, where the Purcell factor $F_{P,1}$ of the dipole mode defined as the ratio of effective density of the SP mode to that of the free space radiation continuum is simply proportional to the square of field enhancement at the Stokes frequency since the mode volume is inversely related to the field intensity; hence, we obtain the well-known but not-so-well-understood E^4 dependence of Raman enhancement.

To simplify the comparison we considered the situation where the optical excitation of the Raman process is the

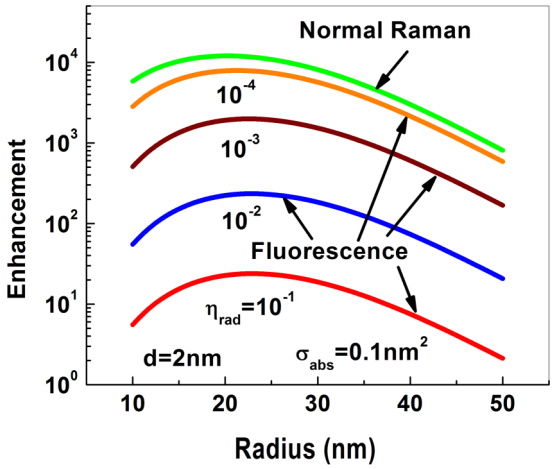

FIG. 5. (Color online) Dependence of enhancement of Raman and fluorescence on the radius of Au nanosphere for a molecule sitting at 2 nm away from the sphere surface. The molecule has absorption cross section of $\sigma_{\rm abs} = 0.1$ nm^2, and its original radiative efficiency $\eta_{\rm rad}$ varies from 10^{-4} to 10^{-1}. Excitation for both processes are at the dipole mode resonance $\omega_{\rm ex} = \omega_1 = 2.562$ eV and emission also at the same Stokes frequency $\omega_S = 2.462$ eV.

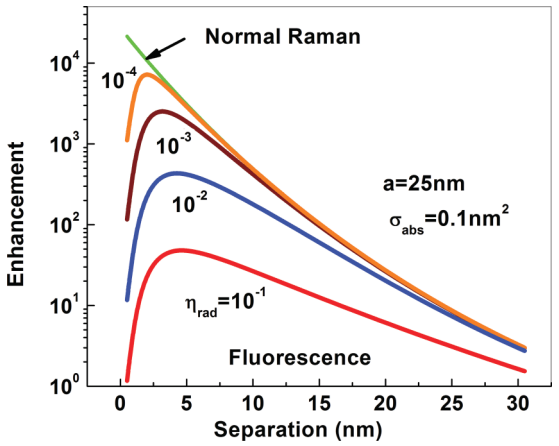

FIG. 6. (Color online) Comparison between Raman and fluorescence enhancement for a range of molecules with $\sigma_{\rm abs} = 0.1$ nm^2 and $10^{-4} \leqslant \eta_{\rm rad} \leqslant 10^{-1}$ for an Au sphere of radius $a = 25$nm.

same as fluorescence at the dipole mode resonance and the Raman Stokes emission has the same shift of 100 meV from its excitation (assuming molecular vibration mode energy of 100 meV). We first illustrate the optimization of the metal nanoparticle size for achieving maximum enhancement. Figure 5 shows the dependence of Raman and fluorescence enhancement on the radius of the metal nanosphere for a fixed separation of 2 nm between the molecule and metal surface. The absorption cross section of the molecule has been fixed at $\sigma_{\rm abs} = 0.1$ nm^2, and its original radiative efficiency varies from 10^{-1} to 10^{-4}. This dependence can be traced to the fact that metal nanoparticles play two mutually exclusive roles: that of antenna for efficient in- and out-coupling of energy and that of a nanocavity for energy concentration. An efficient antenna requires a large size particle with a large dipole, while a high concentration of energy calls for a small particle as nanocavity. Therefore, there exists an optimal size of the particle that is a compromise between the two contradicting requirements. Figure 5 also demonstrates that for a molecule with a small absorption cross section ($\sigma_{\rm abs} = 0.1$ nm^2) as the original radiative efficiency of the molecule $\eta_{\rm rad} \to 0$, the fluorescence enhancement indeed approaches that of Raman.

To illustrate the quenching effect, we fixed the radius of the Au sphere at 25 nm, but varied the spatial separation between the molecule and metal sphere. Figure 6 compares the Raman enhancement to that of fluorescence for a range of molecules with their absorption cross section fixed at $\sigma_{\rm abs} = 0.1$ nm^2 while their original radiative efficiency $\eta_{\rm rad}$ varies from 10^{-4} to 10^{-1}. Not surprisingly, the Raman enhancement consistently outperforms that of fluorescence, which exhibits various degrees of quenching effect depending on the original radiative efficiency, but no quenching whatsoever for Raman process as explained by our model illustrated in Figs. 2(a) and 2(b). Indeed, one can think of Raman process as fluorescence with extremely low efficiency; hence, SP enhancement of Raman enhancement is the absolute upper limit of the fluorescence enhancement.

V. RESONANCE RAMAN ENHANCEMENT

Let us now consider what happens when the excitation frequency $\omega_{\rm ex}$ becomes very close to the molecular resonance ω_m. When the detuning becomes small the broadening γ_m of the molecular transition must be taken into account, and for perfect resonance Eq. (11) becomes

$$\gamma_{\rm RM} = \frac{2\pi}{\hbar}\frac{|d_m E_{\rm ex}|^2}{\hbar^2\gamma_m^2}\frac{|H_{ev}|^2}{\hbar^2(\omega_S-\omega_m)^2}\frac{|d_m|^2\omega_S}{\varepsilon_0}\rho(\omega_S). \qquad (13)$$

For as long as we assume that vibrational frequency is much larger than broadening, the second denominator in Eq. (13) remains nonresonant. The physical reason for the appearance of broadening (or decoherence) γ_m in Eq. (13) is rather simple. As shown in Fig. 2(c), the electric field of the dipole mode at the excitation frequency $\omega_{\rm ex}$ resonantly excites the dipole moment (polarization) of the molecule, $p_m = \mu_{12}\rho_{21}$, where μ_{12} is the matrix element of the $1 \to 2$ transition and ρ_{21} is the density matrix off-diagonal element (often referred to as coherence). In the absence of the metal nanoparticle, polarization decays due to various dephasing processes, such as collisions, interaction with vibrational degrees of freedom, and so on at the dephasing rate of T_2^{-1}, where T_2 is the dephasing or decoherence time. In the presence of metal particles the molecular polarization can decay due to the emission into the higher-order modes at the excitation frequencies, in addition to its original dephasing. While the Raman rate even resonantly enhanced is negligibly small relative to the dephasing rate, the same cannot be said about the SP emission into the higher-order modes at the excitation frequency, especially when the molecule is very close to the surface, and the total dephasing rate (broadening) in the presence of metal nanoparticle increases to

$$\gamma_{m,\rm SP} = \frac{1}{T_2} + \frac{1}{2\tau_{\rm rad}}\sum_{l=1}^{\infty} F_{P,l}(\omega_{\rm ex}), \qquad (14)$$

where the factor of $1/2$ indicates that we are dealing with decay of polarization rather than energy. Thus, the resonance Raman scattering also exhibits quenching by a quenching factor

$$F_{\mathrm{RR},Q} = \frac{\gamma_m}{\gamma_{m,\mathrm{SP}}} = \frac{1}{\left[1 + \frac{T_2}{2\tau_{\mathrm{rad}}} \sum_{l=1}^{\infty} F_{P,l}(\omega_{\mathrm{ex}})\right]^2}. \quad (15)$$

This factor indicates that in the presence of nanoparticles an additional loss channel is introduced for the energy stored in coherent oscillations of molecular dipole at the excitation frequency ω_{ex}. For relatively narrow linewidth molecules placed very close to the metal surface this channel may become comparable in strength to the other dephasing processes, thus suppressing the efficiency of resonance Raman scattering. The total resonance Raman enhancement is thus

$$F_{\mathrm{RR}}(\omega_{\mathrm{ex}},\omega_S) = \frac{1 + \eta_{\mathrm{out}} F_{P,1}(\omega_S)}{\left[1 + \frac{T_2}{2\tau_{\mathrm{rad}}} \sum_{l=1}^{\infty} F_{P,l}(\omega_{\mathrm{ex}})\right]^2} \times \left|\frac{E_{\mathrm{max},1}(\omega_{\mathrm{ex}})}{E_{\mathrm{foc}}}\right|^2 \left(\frac{a}{a+d}\right)^6. \quad (16)$$

Although both experiencing quenching, there is a difference between fluorescence and resonance Raman scattering. In the case of fluorescence, as indicated in Eqs. (8) and (10), the emission into higher-order modes leads to significant quenching when it becomes comparable to the relatively slow relaxation time of the population at the level 2. Hence, the quenching of fluorescence is almost always present. However, in the case of resonance Raman scattering the quenching becomes significant only when emission into the higher-order modes becomes comparable to the much shorter dephasing time T_2; hence, the quenching is observed only for the molecules with narrow absorption spectrum. Of course, resonantly enhanced Raman scattering can be observed only in the molecules with reasonably narrow linewidth; hence, the quenching can indeed be important.

We once again considered the situation where the optical excitation is at the dipole mode resonance, and the Raman

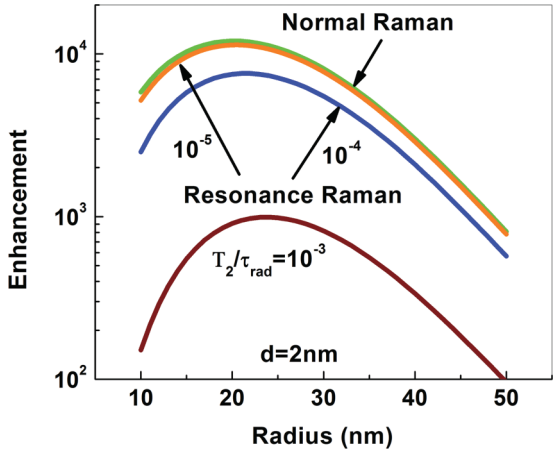

FIG. 7. (Color online) Enhancement of resonance Raman as a function of the radius of Au nanosphere for a molecule sitting at 2 nm away from the metal surface compared to that of normal Raman scattering. The ratio T_2/τ_{rad} of the molecule varies from 10^{-5} to 10^{-3}. Excitation is at the dipole mode resonance $\omega_{\mathrm{ex}} = \omega_1 = 2.562$ eV, and Stokes emission is at $\omega_S = 2.462$ eV.

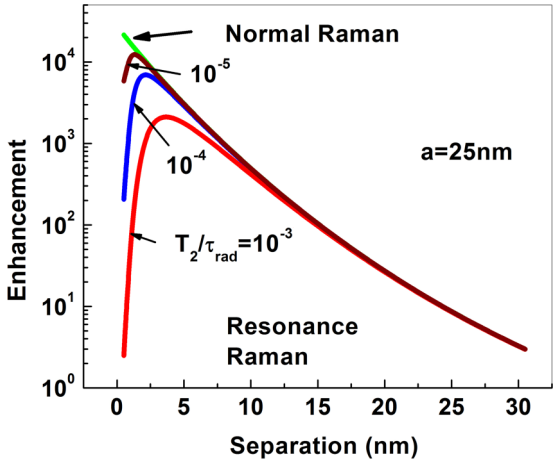

FIG. 8. (Color online) Quenching of resonance Raman for a range of molecules with T_2/τ_{rad} ratio varying from 10^{-5} to 10^{-3} near an Au sphere of radius $a = 25$ nm, compared with normal Raman enhancement.

Stokes emission is red shifted by 100 meV from the excitation. Figure 7 shows the size dependence of the normal and resonance Raman enhancement for a fixed separation of 2 nm between the molecule and metal surface, where the ratio of dephasing time to the radiative lifetime of the molecule has been varied from 10^{-5} to 10^{-3}. Clearly, the resonance Raman enhancement approaches that of normal Raman as $T_2/\tau_{\mathrm{rad}} \to 0$, in which case the molecular absorption spectrum is so broad that resonantly enhanced Raman can no longer be observed.

To illustrate the quenching effect in resonance Raman scattering, we fixed the radius of the Au sphere at 25 nm, but varied the spatial separation between the molecule and metal sphere. Figure 8 compares the resonance Raman enhancement to that of normal Raman for a range of molecules with the ratio T_2/τ_{rad} varying from 10^{-5} to 10^{-3}. As expected, the normal Raman enhancement consistently outperforms that of resonance Raman which exhibits various degrees of quenching as the molecule gets placed closer to the metal nanoparticle, as explained by our model illustrated in Fig. 2(c). Of course, in practice the electronic transitions are often quite broad (the ratio T_2/τ_{rad} can be 10^{-4} or less in organic molecules such as dyes [13,20]), and quenching then becomes barely perceptible, but strictly speaking the quenching is always there.

VI. SUMMARY

It should be noted that in the most rigorous framework the quenching may always take place, because in the vicinity of metal surface there is always a probability that the oscillating dipole will lose its energy to the nonradiative (or nearly nonradiative) SP mode of higher order. That will happen in case of photo (or electro) luminescence, resonance, or nonresonance Raman scattering. This nonradiative decay into higher-order modes is added to the "intrinsic" decay mechanism inside the molecule, and these "intrinsic" mechanisms are dramatically different for different processes. In case of luminescence the intrinsic decay is defined by nonradiative relaxation time τ_{nrad} inside the molecule which can be quite

slow; hence, nonradiative decay into higher-order modes can greatly increase total nonradiative decay, and quenching especially for a molecule with high radiative efficiency is significant. In case of resonance Raman scattering the intrinsic decay is defined by the dephasing rate T_2^{-1}, which, as a rule, is much faster than $1/\tau_{\text{nrad}}$; therefore, the nonradiative decay into higher-order modes can only slightly increase total nonradiative decay and the quenching is much weaker than for fluorescence. Finally, for the nonresonance Raman scattering the decay rate of virtual state is defined by detuning $\omega_{\text{ex}} - \omega_m$ and is so fast that the nonradiative decay into higher-order modes pales in comparison, and no matter how close to the surface is the molecule, practically no quenching ensues.

Thus, from the practical point of view, we have presented a physically transparent analytical model for a comparative study of the enhancement of fluorescence, normal nonresonance Raman, and resonance Raman processes near metal nanoparticles. We have confirmed and explained the fundamental difference that makes normal Raman enhancement typically much stronger than fluorescence enhancement. We have shown that, unlike fluorescence, nonresonance Raman process does not get quenched at the surface. In addition, we have also analyzed the enhancement of resonance Raman scattering and showed that for molecules with reasonably narrow linewidth on which the resonantly enhanced Raman can be observed, quenching can indeed take place as well, although never as drastic as for fluorescence.

For experimentalists our results indicate that the spectacular SERS-like enhancement of fluorescence is unattainable except for the molecules whose original luminescence efficiency is very low and show how this limited enhancement can be optimized. Similarly, when one tries to take advantage of resonance in Raman process, the enhancement in the vicinity of metal surface is not as strong as for the nonresonance Raman and needs to be optimized. All these results confirm the most general truism that SP enhancement is most spectacular for the processes that have the lowest original efficiency, and the absolute efficiency of the enhanced process remains relatively low; hence, the applications that do not require high absolute efficiency, such as SERS, stand the most to benefit.

ACKNOWLEDGMENT

This work is sponsored in part by the Air Force Office of Scientific Research under Grant No. FA9550-10-1-0417.

[1] S. Kühn, U. Håkanson, L. Rogobete, and V. Sandoghdar, Phys. Rev. Lett. **97**, 017402 (2006).
[2] L. Novotny, Appl. Phys. Lett. **69**, 3806 (1996).
[3] S. Kühn, G. Mori, M. Agio, and V. Sandoghdar, Mol. Phys. **106**, 893 (2008).
[4] P. Bharadwaj and L. Novotny, Opt. Express **15**, 14266 (2007).
[5] R. Bardhan, N. K. Grady, J. R. Cole, A. Joshi, and N. J. Halas, ACS Nano **3**, 744 (2009).
[6] H. Wei, Z. Li, X. Tian, Z. Wang, F. Cong, N. Liu, S. Zhang, P. Nordlander, N. J. Halas, and H. Xu, Nano Lett. **11**, 471 (2011).
[7] M. Moskovits, Rev. Mod. Phys. **57**, 783 (1985).
[8] M. Moskovits, L. Tay, J. Yang, and T. Haslett, Top. Appl. Phys. **82**, 215 (2002).
[9] K. Kneipp, Y. Wang, H. Kneipp, L. T. Perelman, I. Itzkan, R. R. Dasari, and M. S. Feld, Phys. Rev. Lett. **78**, 1667 (1997).
[10] S. Nie and S. R. Emory, Science **275**, 1102 (1997).
[11] A. M. Michaels, M. Nirmal, and L. E. Brus, J. Am. Chem. Soc. **121**, 9932 (1999).
[12] Z. Wang, S. Pan, T. D. Krauss, H. Dui, and L. J. Rothberg, Proc. Natl. Acad. Sci. USA **100**, 8638 (2003).
[13] E. C. Le Ru and P. G. Etchegoin, *Principles of Surface Enhanced Raman Spectroscopy and Related Plasmonic Effects* (Elsevier, Amsterdam, 2009).
[14] R. Acevedo, R. Lomardini, N. J. Halas, and B. R. Johnson, J. Phys. Chem. A **113**, 13173 (2009).
[15] A. Barhoumi, D. Zhang, F. Tam, and N. J. Halas, J. Am. Chem. Soc. **130**, 5523 (2008).
[16] M. Fleischmann, P. J. Hendra, and A. J. McQuillan, Chem. Phys. Lett. **26**, 163 (1974).
[17] D. A. Weitz, S. Garoff, J. I. Gersten, and A. Nitzan, J. Chem. Phys. **78**, 5324 (1983).
[18] R. M. Bakker, V. P. Drachev, Z. Liu, H.-K. Yuan, R. H. Pedersen, A. Boltasseva, J. Chen, J. Irudayaraj, A. V. Kildishev, and V. M. Shalaev, New J. Phys. **10**, 125022 (2008).
[19] S. A. Meyer, E. C. Le Ru, and P. G. Etchegoin, J. Phys. Chem. A **114**, 5515 (2010).
[20] C. M. Galloway, P. G. Etchegoin, and E. C. Le Ru, Phys. Rev. Lett. **103**, 063003 (2009).
[21] E. Dulkeith, A. C. Morteani, T. Niedereichholz, T. A. Klar, J. Feldmann, S. A. Levi, F. C. J. M. vanVeggel, D. N. Reinhoudt, M. Moller, and D. I. Gittins, Phys. Rev. Lett. **89**, 203002 (2002).
[22] B. Pettinger, J. Chem. Phys. **85**, 7442 (1986).
[23] H. Xu, X.-H. Wang, M. P. Persson, H. Q. Xu, M. Käll, and P. Johansson, Phys. Rev. Lett. **93**, 243002 (2004).
[24] R. Carminati, J.-J. Greffet, C. Henkel, and J. M. Vigoureux, Opt. Commun **261**, 368 (2006).
[25] A. M. Kern and O. J. F. Martin, Nano Lett. **11**, 482 (2011).
[26] G. Sun, J. B. Khurgin, and A. Bratkovsky, Phys. Rev. B **84**, 045415 (2011).
[27] G. Sun, J. B. Khurgin, and R. A. Soref, Appl. Phys. Lett. **94**, 101103 (2009).
[28] G. Sun, J. B. Khurgin, and C. C. Yang, Appl. Phys. Lett. **95**, 171103 (2009).
[29] P. G. Etchegoin, E. C. Le Ru, and M. Meyer, J. Chem. Phys. **125**, 164705 (2006).
[30] P. B. Johnson and R. W. Christy, Phys. Rev. B **6**, 4370 (1972).
[31] J. B. Khurgin and G. Sun, Appl. Phys. Lett. **99**, 211106 (2011).
[32] R. W. Boyd, *Nonlinear Optics*, 2nd ed. (Academic Press, San Diego, 2003), p. 169